

Electrochemical Formation of Chiral Polyaniline Colloids Codoped with (+)- or (–)-10-Camphorsulfonic Acid and Polystyrene Sulfonate

Peter C. Innis, Ian D. Norris, Leon A. P. Kane-Maguire,* and Gordon G. Wallace*

Intelligent Polymer Research Institute, Department of Chemistry, University of Wollongong, Northfields Avenue, Wollongong, NSW 2522, Australia

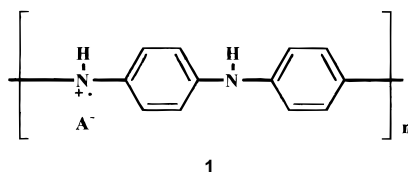
Received November 4, 1997; Revised Manuscript Received July 14, 1998

ABSTRACT: Chiral polyaniline colloids have been generated via the electrohydrodynamic polymerization of aniline in aqueous (+)- or (–)-10-camphorsulfonic acid (HCSA) using polystyrene sulfonate (PSS) as a steric stabilizer and codopant. Potentiostatic polymerization at +0.9 V (vs Ag/AgCl) was employed. The colloidal PAN·HCSA/PSS dispersions produced after various electropolymerization periods (30–90 min) became optically active upon aging over 24 h, revealing mirror-imaged circular dichroism (CD) spectra for PAN·(+)-HCSA/PSS and PAN·(–)-HCSA/PSS samples. This indicated an enantioselective rearrangement of the polyaniline chains induced by the chiral HCSA dopants after the initial electropolymerization and acid doping. Dialyzed colloidal dispersions were stable for extended periods (6 months) and revealed particles with a mean size of 180 ± 10 nm, although particles were observed at up to 1000 nm. Similar particles were observed by TEM studies. Chemical dedoping with ammonia of films cast from these dispersions yielded the optically active emeraldine base form of the polymer, while reduction with hydrazine gave the corresponding leucoemeraldine base.

Introduction

Due to its high environmental stability, facile redox and pH switching between differently colored states, relatively high conductivity, and low cost, polyaniline (PAN) is recognized as one of the most promising organic conducting polymers for future commercialization. A wide range of potential applications are being explored, including use as electrochromic devices,¹ rechargeable batteries,² sensors,³ catalysts,⁴ electrochemical capacitors,⁵ and anti-corrosion agents,⁶ as well as use in electrochromatography.⁷

There has also been considerable recent interest in chiral conducting polyanilines because of their potential use in areas such as electrochemical asymmetric synthesis, chiral chromatography, and membrane separation technology. The first such chiral polyaniline salts, namely **1** {HA = (+)- or (–)-camphorsulfonic acid



(HCSA)}, were prepared as films in our laboratories via the electropolymerization of aniline in the presence of (+)- or (–)-HCSA, respectively.⁸ It has been subsequently shown that related optically active salts can also be generated in solution⁹ and as films^{10,11} by the acid doping of emeraldine base (EB) with (+)- or (–)-HCSA in various organic solvents.

Interestingly, Minto and Vaughan¹² have recently reported that a film of optically active PAN·(+)-HCSA salt cast from *m*-cresol exhibits four times the conductivity of the corresponding salt with racemic (±)-HCSA. X-ray diffraction data indicated enhanced stereoregularity and crystallinity in the salt containing the homochiral (+)-HCSA dopant. Chiral PAN·(+)-HCSA

membranes have also shown¹³ considerable chiral discrimination in the electrochemically activated transport of enantiomeric (+)-CSA[–] and (–)-CSA[–] ions.

An important factor that has to date limited some of the potential commercial applications of polyanilines has been their intractability. However, several recent advances have significantly enhanced their processability. These include the discovery that the conducting emeraldine salt form of PAN·HA can be readily solubilized in a range of organic solvents via the use of surfactant-like dopant acids (HA) such 10-camphorsulfonic acid and dodecylbenzenesulfonic acid.^{14,15} A major goal of recent studies has been to achieve water soluble or dispersible polyanilines. One approach has been by the incorporation of ionisable sulfonic acid groups onto the aniline rings or the aniline nitrogen atom, either pre- or post-polymerization, to produce self-doped polymers.^{16–18} Similarly, water-soluble polyanilines bearing carboxylic acid ring substituents have also been reported.¹⁹

An alternate approach, which has been successful with the unsubstituted parent polyaniline, is the formation of colloidal dispersions of polyaniline via chemical oxidation, using a range of steric stabilizers.^{20–24} Another recent route to water solubilization involves mixing high molecular weight poly(4-styrenesulfonic acid) (PSS) with aniline to form a block copolymer, stabilized by strong hydrogen and ionic bonding to form a doped water-dispersible complex.²⁵

The above paths to achiral colloidal polyaniline dispersions have all involved chemical oxidation or secondary processing treatments. In this paper, we report the electrosynthesis of chiral conducting polyaniline salts in the form of water soluble colloidal dispersions, via a novel electro-hydrodynamic technique²⁶ developed in our laboratory. Major advantages of this technique over chemical routes include (i) greater quantitative control over the oxidation process and (ii) the wider range of counterions that can be incorporated into the polymer at the synthesis stage, rather than as a postsynthesis process.

* To whom correspondence should be addressed.

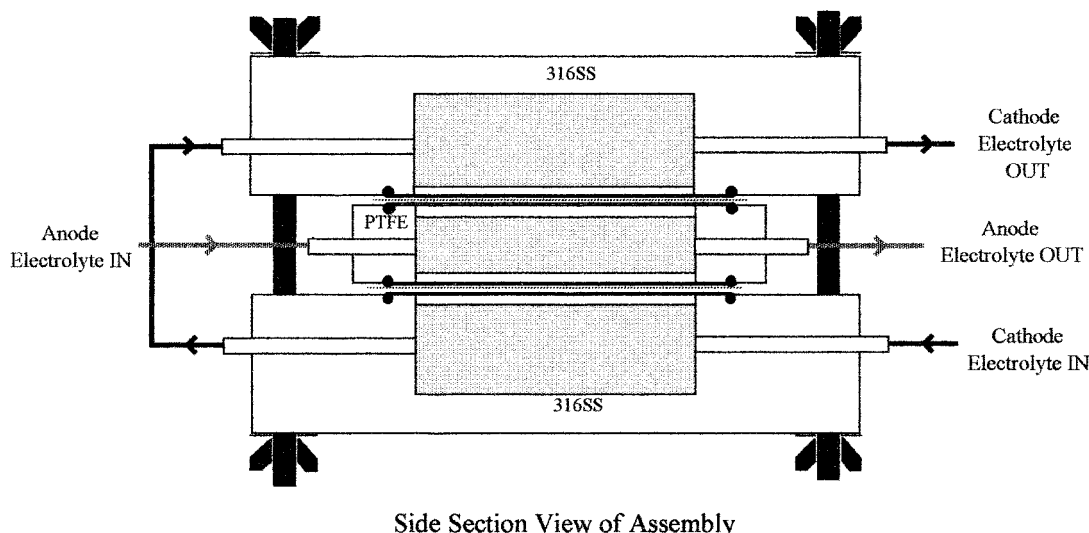


Figure 1. Electrochemical flow-through cell.

In the current study, optically active polyaniline colloidal salts of the type $\text{PAn}\cdot(+)\text{-HCSA/PPS}$ and $\text{PAn}\cdot(-)\text{-HCSA/PPS}$ have been generated via the potentiostatic polymerization of aniline, utilizing PSS as a steric stabilizer and codopant. The chiroptical and electrical properties of these chiral colloids are described, both as aqueous dispersions and as films, as well as their chemical reactivity. They are seen to be considerably more stable than related chiral $\text{PAn}\cdot\text{HCSA/PEO}$ colloids that we recently briefly reported,²⁷ where poly(ethylene oxide) was employed as a steric stabilizer.

Experimental Section

Materials. Aniline (BDH) was distilled and stored under $\text{N}_2(\text{g})$ prior to use. Poly(styrenesulfonic acid) (PSS) (sodium salt, MW 70 000), (1*S*)-(+)- and (1*R*)-(-)-10-camphorsulfonic acid (HCSA), and hydrazine dihydrate were purchased from Aldrich Chemical Co. Sodium nitrate, concentrated sulfuric acid, and concentrated ammonia were purchased from Ajax Ltd. (Univar) and used as supplied.

Electrochemical Polymerization. Aniline polymerization was performed in a divided electrochemical flow-through cell, shown in Figure 1. The anode and cathode consisted of porous reticulated vitreous carbon (RVC), with a porosity of 100 pores per inch (PPI) and an effective surface area of $65.6 \text{ cm}^2/\text{cm}^3$ (ERG Materials and Aerospace Corp.). The anode RVC disk was separated from the two cathodes by an ion exchange membrane (Neosepta AMH A-2119, Tokuyama Corp.) to prevent mixing of the anolyte and catholyte solutions. Two cathode disks ($20 \times \text{o.d. } 50 \text{ mm}$, 2576 cm^2) were employed on the opposite faces of the anode ($15 \times \text{o.d. } 50 \text{ mm}$, 1932 cm^2) to give uniform electric field distribution.

An anode synthesis solution (500 mL) was prepared containing $0.25 \text{ mol dm}^{-3} \text{ H}_2\text{SO}_4$, 0.25 mol dm^{-3} aniline, 0.2 mol dm^{-3} (+)- or (-)-HCSA and 3 g/L PSS (1.50 g), together with a separate cathode solution (500 mL) containing $0.5 \text{ mol dm}^{-3} \text{ NaNO}_3$. These electrolyte solutions were passed through their respective compartments at a flow rate of 165 mL/min by a peristaltic pump. Electropolymerization was carried out at $+0.90 \text{ V vs Ag/AgCl}$ for a total of 90 min. Aliquots (ca. 20 mL) were withdrawn at 30 min intervals, and their UV-visible and circular dichroism (CD) spectra were recorded.

The colloidal dispersions formed after 90 min were then dialyzed for 24 h using cellulose membrane dialysis tubing with a molecular weight cutoff greater than 12 000 (Sigma) to remove excess aniline monomer, HCSA and H_2SO_4 . Separate studies with aqueous PSS solutions indicated that dialysis under these conditions also removed $17 \pm 1\%$ of this polyelectrolyte.

Particle Size Analysis. The particle size and mobility analysis of the above dialyzed colloidal dispersions were carried out using a Malvern Zetamaster PCS.

Film Formation. Thin films of $\text{PAn}\cdot(+)\text{-HCSA/PSS}$ were prepared by concentrating ca. 400 mL of the dialyzed colloidal dispersions to ca. 25 mL by rotary evaporation at 45°C . Approximately 0.5 mL portions of this solution were then cast onto glass slides via pipet and dried at 60°C to produce thin, green films of the $\text{PAn}\cdot(+)\text{-HCSA/PSS}$ salt suitable for chiroptical and chemical dedoping and redox studies.

Spectroscopic Studies. UV-visible spectra of the aliquots sampled after various electropolymerization times were recorded from 300 to 1100 nm using a Shimadzu UV1601 spectrophotometer. These were measured in a 10 mm cuvette after diluting 250 μL of sample in 1.25 mL of milli-Q grade water. Circular dichroism spectra (Jobin Yvon Dichrograph 6) were measured from 330 to 700 nm by diluting 1.0 mL of sample in 1.50 mL of milli-Q grade water, using a 10 mm path length cell. UV-visible and CD spectra were also recorded for these samples after further standing for various periods (1–7 days) in sealed containers. CD and UV-visible spectra were similarly measured for films of $\text{PAn}\cdot(+)\text{-HCSA/PSS}$ evaporatively deposited from the above colloidal dispersions.

Microscopy Studies. Tunneling electron microscopy (TEM) measurements were performed on the dialyzed dispersions doped with either (+)- or (-)-HCSA on a JEOL 2000 TEM (80 kV), by evaporating a drop of the solution onto a 300 mesh Lacey Carbon (Type A) Copper TEM grid (Pelco Int.). In situ electron diffraction studies were also performed on individual colloid particles to investigate the occurrence of crystallinity, as well as to confirm the identities of the TEM image features.

Electrochemical Studies. Cyclic voltammetry studies on the dialyzed concentrate of the $\text{PAn}\cdot(+)\text{-HCSA/PSS}$ colloid were performed using a PAR 273A potentiostat. The potential was cycled between -0.2 and $+1.0 \text{ V vs Ag/AgCl}$ at a scan rate of 50 mV/s.

Results and Discussion

(a) Chiral $\text{PAn}\cdot(+)\text{-HCSA/PSS}$ and $\text{PAn}\cdot(-)\text{-HCSA/PSS}$ Colloids. (i) Formation. The hydrodynamic electropolymerization of aniline at $+0.9 \text{ V vs Ag/AgCl}$ in the presence of $0.25 \text{ mol dm}^{-3} \text{ H}_2\text{SO}_4$, 0.2 mol dm^{-3} (+)- or (-)-HCSA, and 3 g/L PSS as a steric stabilizer generated a deep green anolyte "solution". UV-visible spectra of aliquots taken at 30 min intervals exhibited absorption bands at ca. 385 and 775 nm, characteristic of an emeraldine salt (Figure 2). Although solutions of $\text{PAn}\cdot\text{HA}$ salts in organic solvents typically show both a localized polaron band (ca. 440 nm) and a $\pi\text{-}\pi^*$ band

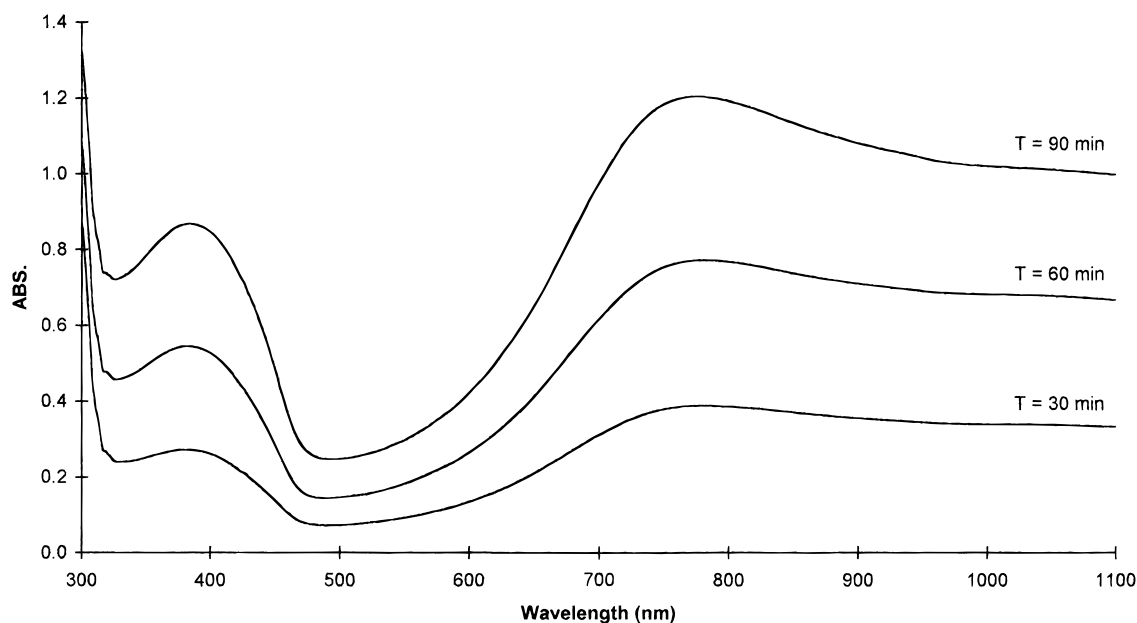


Figure 2. UV-visible spectra of PAN·(-)-HCSA/PSS colloidal dispersions sampled after various electropolymerization times (T) (diluted $\times 6$).

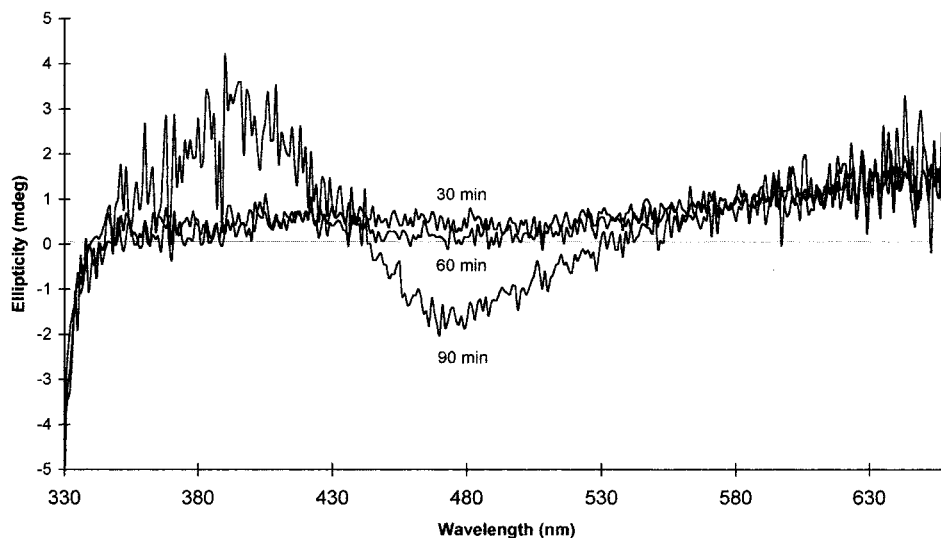


Figure 3. CD spectra of PAN·(-)-HCSA/PSS colloidal dispersion immediately after sampling from electrosynthesis cell ($T = 30$ – 90 min).

(ca. 350 nm) in the low wavelength region,¹¹ films can exhibit²⁸ a single broad band as observed for our colloids. The intensity of the 385 and 775 nm bands increased with polymerization time over a 90 min period, indicating a progressive increase in concentration of the emeraldine salt formed. These results, together with the "solubility" in water, are consistent with the formation of colloids of the type PAN·(+)-HCSA/PSS and PAN·(-)-HCSA/PSS, where PSS acts not only as a steric stabilizer but also as a competitive dopant for the formation of the emeraldine salt.

The UV-visible spectra of the individual aliquots changed only slightly over a 24 h period, confirming the generation of stable colloidal dispersions. Quantitatively similar UV-visible spectra, which were also stable for extended periods, were obtained after dialysis of these dispersions for 24 h to remove excess aniline monomer, HCSA and H₂SO₄.

Following dialysis of a 90 min reaction sample, 1.53 ± 0.03 g of PAN·(+)-HCSA/PSS colloid was recovered.

After correction for the PSS estimated to be lost during dialysis (17%) this reduces to a mass of 0.29 ± 0.01 g of PAN·(+)-HCSA produced in the total synthesis volume (500 mL). This is substantially higher than that reported by us for PAN·PEO/HCSA colloids prepared with an earlier, less efficient flow-through cell.²⁷

(ii) Chiroptical Properties of PAN·(+)- and (-)-HCSA/PSS Colloids. Circular dichroism (CD) spectra of samples of the above PAN·(+)- and (-)-HCSA/PSS colloids withdrawn after 30 and 60 min electropolymerization revealed no significant optical activity (Figure 3). However, samples withdrawn after 90 min exhibited broad CD bands at ca. 390 and 465 nm. These visible bands are clearly associated with the macro-asymmetry of the polyaniline chains, rather than the presence of the chiral (+)- and (-)-HCSA dopants, which only have CD signals in the UV region (ca. 290 nm). The 390 and 465 nm CD peaks may be assigned as the exciton-coupled bands associated with the polyaniline absorption band at ca. 410 nm (Figure 7). The CD band(s)

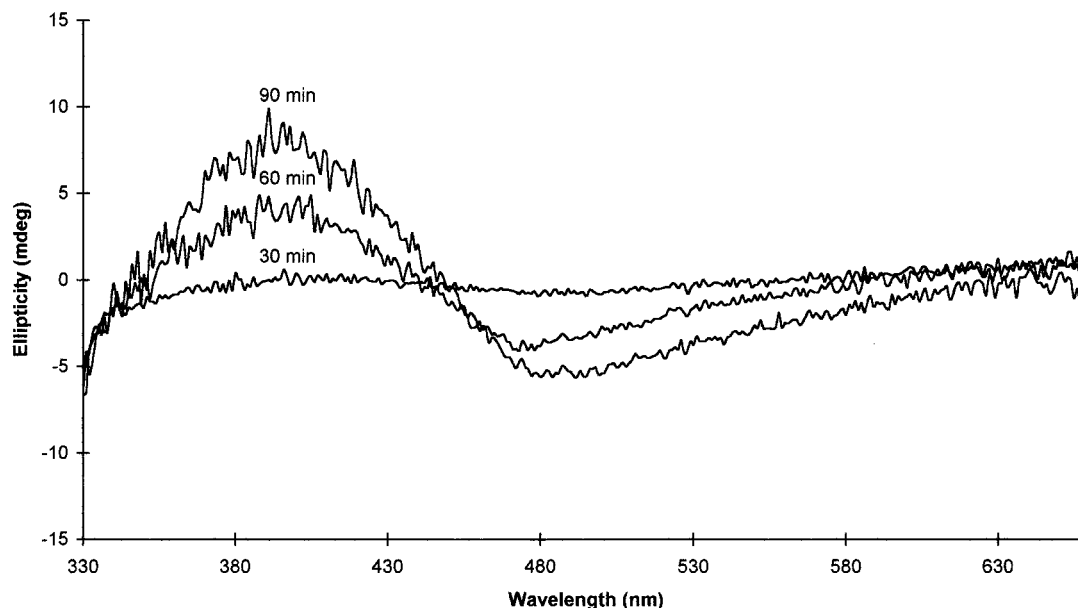


Figure 4. CD spectra of PAN·(-)-HCSA/PSS colloidal dispersions after aging for 24 h.

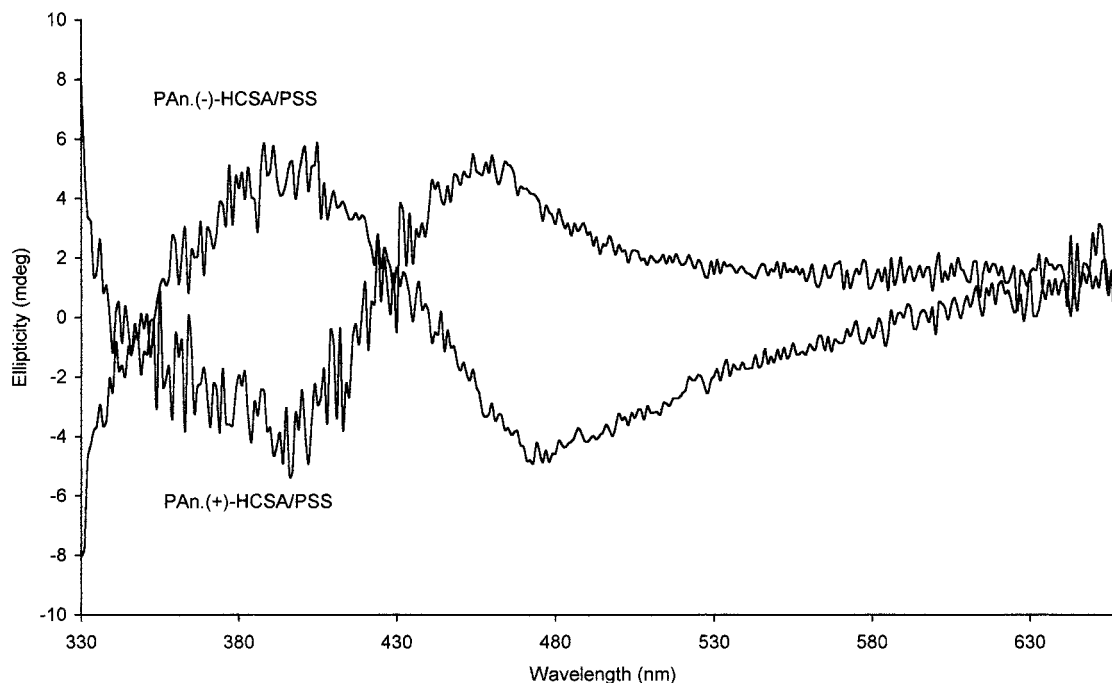


Figure 5. CD spectra of PAN·(+)-HCSA/PSS and PAN·(-)-HCSA/PSS colloid aged for 24 h after 90 min electrosynthesis.

associated with the localized polaron absorption band at ca. 800 nm could not be recorded, due to instrumentation limitations at these longer wavelengths.

The CD spectra of all the PAN·HCSA/PSS colloid samples increased markedly in intensity over 24 h (Figure 4), although their UV–visible spectra remained constant. This indicates that the optical activity in the colloids arises from an asymmetric rearrangement of the polyaniline chains after the initial doping process. A similar conclusion has been previously drawn from chiroptical studies of the doping of the emeraldine base form of poly(*o*-toluidine) with (+)-HCSA in DMF solvent.¹¹

The CD spectra of the PAN·(+)-HCSA/PSS and PAN·(-)-HCSA/PSS colloids were mirror imaged, indicating an enantioselective induction of chirality in the polyaniline chains caused by the chiral HCSA dopants

(Figure 5). Interestingly, the observed CD spectra are distinctly different to those reported for optically active PAN·(+)-HCSA and PAN·(-)-HCSA films potentiostatically deposited on ITO-coated glass electrodes in a static electrochemical cell.⁸ However, they are similar in band position and sign to those observed when the latter PAN·HCSA salts are generated by doping emeraldine base (EB) with (+)- or (-)-HCSA in organic solvents (e.g. bands at 400 and 450 nm in DMSO).¹¹ This suggests that the polyaniline chains in the PAN·HCSA/PSS colloids are largely in a compact coil conformation. This is supported by the corresponding absorption spectra (Figure 2), which exhibit a localized polaron band at 775 nm. However the presence also of a partial free-carrier tail absorbance in the near infrared region suggests that some chains are also in an extended coil conformation.

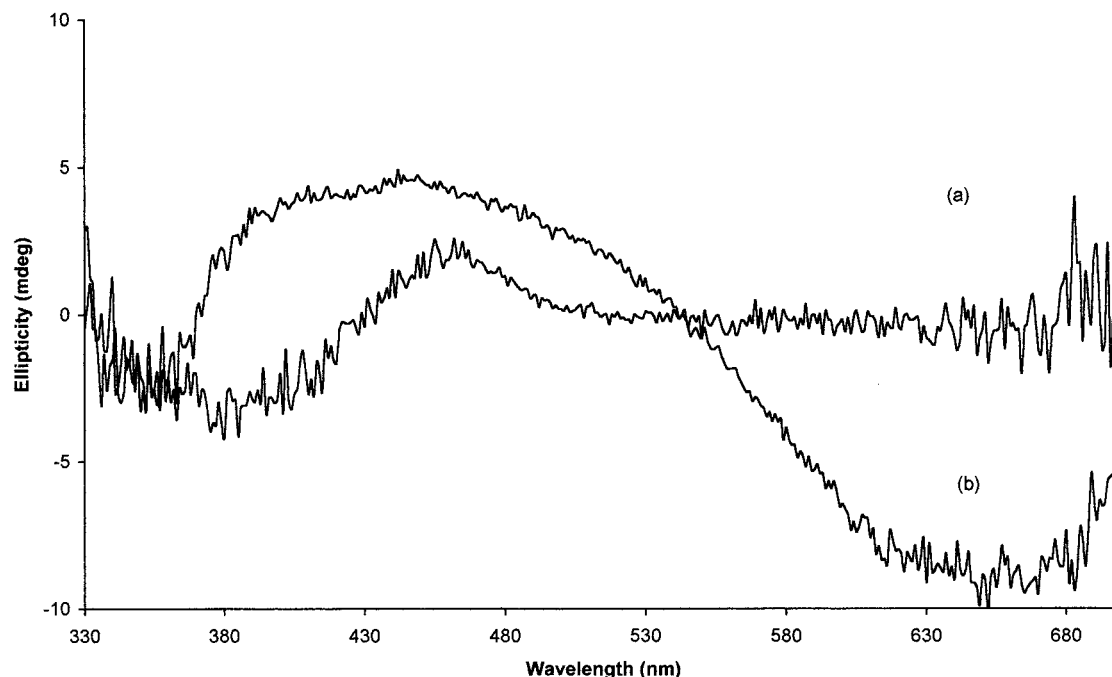


Figure 6. (a) CD spectrum of PAn·(+)-HCSA/PSS colloid cast as a film onto glass. (b) CD spectrum after exposure to NH_3 vapor to form an EB film.

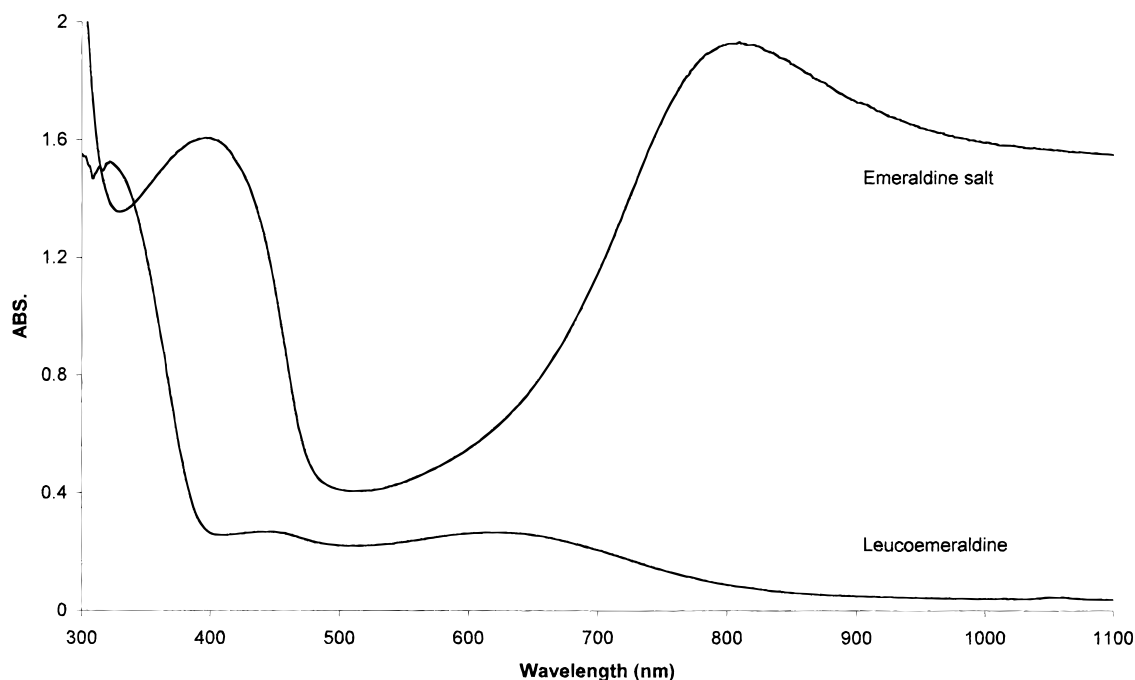


Figure 7. UV-visible spectrum of PAn·(+)-HCSA/PSS colloid cast as a film and exposed to hydrazine to form leucoemeraldine.

The CD spectra of the aqueous PAn·HCSA/PSS colloidal dispersions were not significantly altered after subsequent dialysis for 24 h. Further concentration of these dialyzed colloidal dispersions, followed by evaporative casting, gave films that exhibited similar UV-visible (Figure 7) and CD (Figure 6a) spectra to their parent dispersions. This indicated similar conformations for the polyaniline chains in both solid (film) and aqueous dispersions. The identical λ_{max} (775 nm) for the localized polaron absorption band in both cases also suggested similar conjugation lengths for the polyaniline chains.

(iii) Dedoping of the PAn·(+)-HCSA/PSS and PAn·(-)-HCSA/PSS Films. Exposure of the green

film cast from an aqueous PAn·(+)-HCSA/PSS dispersion to ammonia vapor led to its rapid dedoping to the blue emeraldine base (EB) form. This was confirmed by the disappearance of the localized polaron band of the emeraldine salt at 775 nm and the appearance of λ_{max} at 330 and 600 nm characteristic of EB. The corresponding CD spectrum (Figure 6b) was similar to that recently reported²⁹ for EB produced via the dedoping of PAn·(+)-HCSA films with aqueous NH_4OH .

Upon further standing in air (20 min), the film returned to its initial green color due to the loss of the NH_3 vapor, and the CD spectrum of the emeraldine salt colloid (PAn·(+)-HCSA/PSS) was quantitatively recovered. This dedoping/redoping sequence could be re-

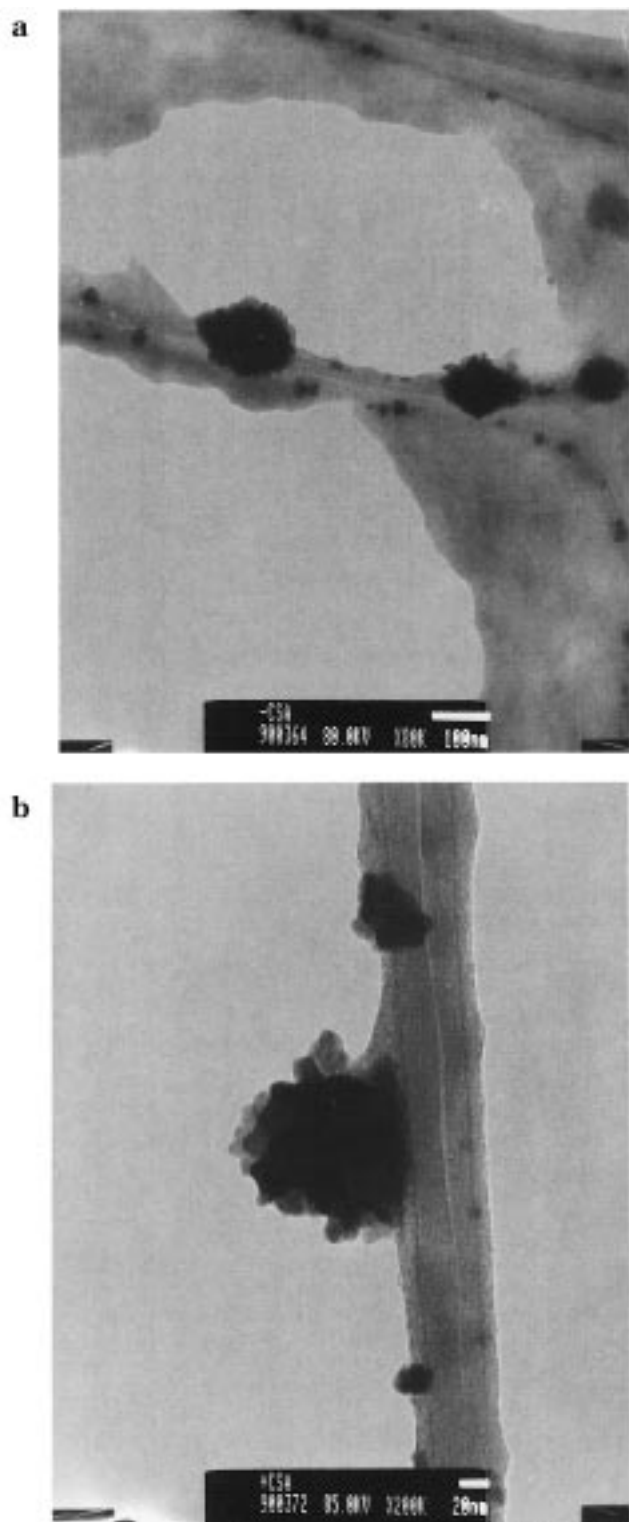


Figure 8. TEM of PAN·(-)-HCSA/PSS colloid at (a) 80 000 magnification, and (b) 200 000 magnification.

peated over several cycles without apparent deterioration of the film.

(iv) Reduction to Colloidal Leucoemeraldine (LB). Addition of 1 drop of an aqueous solution of hydrazine to a colloidal PAN·(+)-HCSA/PSS film caused rapid (seconds) dedoping to give blue EB, followed by slower (minutes) reduction to give the pale yellow color characteristic of leucoemeraldine base (LB). The formation of the leucoemeraldine base was confirmed by the



Figure 9. Electron diffraction pattern of PAN·(-)-HCSA particle in a PAN·(-)-HCSA/PSS colloid.

disappearance of the initial visible region absorption bands and their replacement by the characteristic UV band of LB at 320 nm (Figure 7). As expected, this colloidal leucoemeraldine film exhibited no visible region CD bands.

(v) TEM, Electron Diffraction Analysis, and Particle Size Analysis. Colloid particles were imaged by TEM. In Figure 8a, colloid particles of PAN·(+)-HCSA/PSS were observed as dark spherical features that stick to the surfaces of the TEM lacey grid. The larger particles (100 nm), also shown at a higher magnification in Figure 8b, are clearly aggregate structures of the smaller colloid particles ca. 10–20 nm in size. The void spaces between the TEM grid were seen to be bridged by the excess PSS (Figure 8a). Further identification of these image features was derived from electron diffraction measurements on the PSS and PAN·(+)-HCSA/PSS particles. The broad ill-defined diffraction pattern for the bridging PSS material indicated an amorphous character. In contrast, a PAN·(+)-HCSA/PSS colloid particle (Figure 9) exhibited a distinct crystalline diffraction pattern similar to those reported for aligned fibers of PAN·HCSA cast from *m*-cresol.^{30,31}

Particle size and mobility analysis of colloidal dispersions of PAN·(+)-HCSA/PSS (90 min) were also carried out using a Malvern Zetamaster PCS. This technique is based upon laser light scattering, which is dependent upon the size of a particle that is assumed to be spherical. Particles smaller than 100 nm could not be detected by this instrument. The mean particle size for the colloids were observed to be 180 ± 10 nm, in a skewed distribution with a broad particle size tail at up to 1000 nm. The presence of the larger particles indicated the presence of some macroscopic colloid aggregation. The ζ potential of the colloids was -45 ± 4 mV, with an average mobility of -3.2 ± 0.3 cm² s⁻¹ V⁻¹ A⁻¹. These results are consistent with the use of the negatively charged PSS as a stabilizer.

Electrochemical Characterization. The cyclic voltammogram (second scan) of a dialyzed concentrate

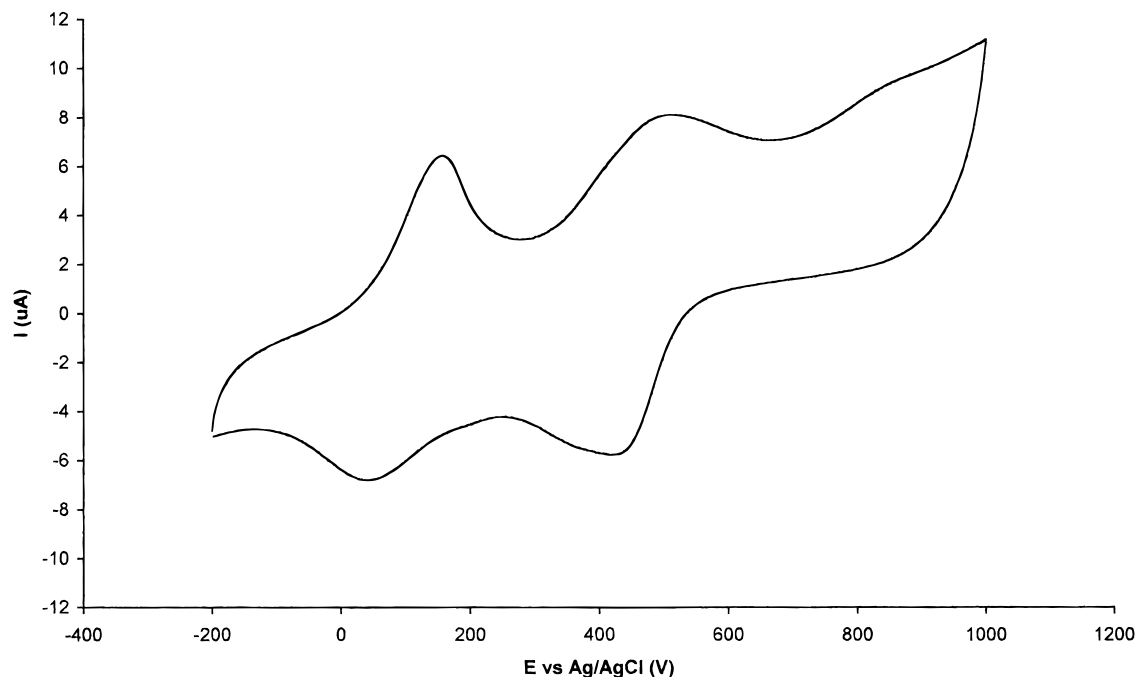


Figure 10. Cyclic voltammogram of PAN·(+)-HCSA/PSS colloidal dispersion on a Pt disk electrode (scan rate 50 mV/s).

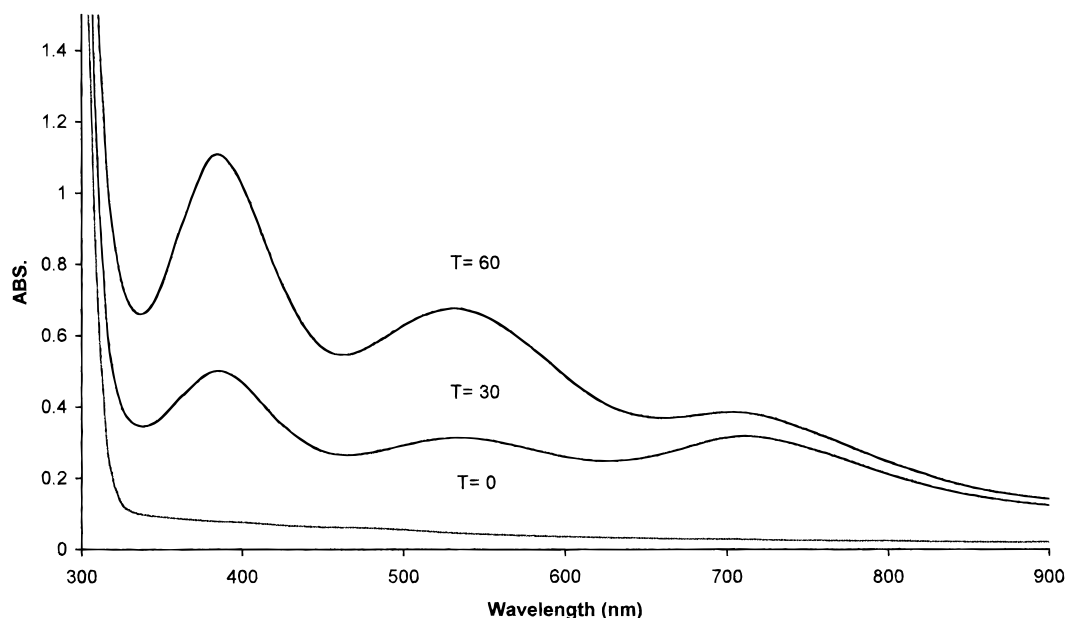


Figure 11. UV-visible spectrum of PAN·(±)-HCSA/PEO colloidal dispersions sampled after various electropolymerization times (T).

of the PAN·(+)-HCSA/PSS colloid on a 1.5 mm platinum disk electrode is shown in Figure 10. This displays two reversible redox responses similar to those reported for PAN·HCSA films. The oxidation peak at 0.155 V may be assigned to the conversion of leucoemeraldine to emeraldine salt, while the peak at 0.515 V corresponds to the subsequent oxidation to the pernigraniline form.

(b) PAN·(+)-HCSA/PEO and PAN·(-)-HCSA/PEO Colloids. Related chiral, colloidal dispersions of the type PAN·(+)-HCSA/PEO and PAN·(-)-HCSA/PEO were also obtained by electropolymerizing aniline (0.1 mol dm⁻³) using the same flow-through cell in the presence of 0.25 mol dm⁻³ H₂SO₄, 0.1 mol dm⁻³ (+)-HCSA, and 3.5 g/L poly(ethylene oxide) (PEO) as a steric stabilizer. Their UV-visible spectra (Figure 11) displayed three peaks at 286, 535, and 712 nm. The absorption at 535

nm is typical of the fully oxidized pernigraniline form of polyaniline, indicating considerable over-oxidation of the colloidal polyaniline. Less extensive over-oxidation was also evident in the polyaniline colloids reported previously by us from electropolymerizing aniline in solutions of HCl with PEO as steric stabilizer.²⁷ In these earlier experiments, a flow-through cell of substantially lower electrochemical efficiency was employed. In addition, polyaniline dispersions formed using PEO as steric stabilizer were relatively unstable, coagulating on standing. Our current studies therefore show that PSS is superior to PEO as a stabilizer for electrochemically produced polyaniline colloids.

Conclusions

Optically active polyaniline colloids can be readily prepared via the electrohydrodynamic polymerization

of aniline in aqueous sulfuric acid containing an enantiomer of 10-camphorsulfonic acid (HCSA), as well as polystyrene sulfonic acid as a stabilizer and codopant. The optical activity increases upon standing for 24 h, indicating an asymmetric rearrangement of the polyaniline chains induced by the chiral HCSA. The colloidal dispersions are stable for several months. Deposing of films cast from these colloidal dispersions with ammonia vapor provided a route to optically active emeraldine base.

Acknowledgment. Ms. V. Aboutanos is thanked for assistance with colloid particle sizing and Mr. L. Brunckhorst for TEM measurements. We are grateful to the Australian Research Council for support.

References and Notes

- (1) Monkman A. P. In *The Encyclopedia of Advanced Materials*, Bloor, D., Brook, R. J., Flemings, M. C., Mahajan, M. C., Eds.; Elsevier: Cambridge, U.K., 1994; Vol. 1, p 668.
- (2) Barbero, C.; Miras, M. C.; Koetz, R.; Haas, O. *Synth. Met.* **1993**, *55*, 1539 and references cited therein.
- (3) Barisci J. N.; Conn, C.; Wallace, G. G. *Trends Polym. Sci.* **1996**, *4*, 307.
- (4) Higuchi, M.; Ikeda, I.; Hirao, T. *J. Org. Chem.* **1997**, *62*, 1072 and references cited therein.
- (5) Roth, S.; Graupman, W. *Synth. Met.* **1993**, *55–57*, 3623.
- (6) DeBerry D. W. *J. Electrochem. Soc.* **1985**, *13*, 1022.
- (7) (a) Ge, H.; Teasdale, P. R.; Wallace G. G. *J. Chromatogr.* **1991**, *544*, 305. (b) Nagaoka, T.; Kakuno K.; Fujimoto, M.; Nakao, H.; Yano, J.; Ogura, K. *J. Electroanal. Chem.* **1994**, *368*, 315.
- (8) Majidi, M. R.; Kane-Maguire, L. A. P.; Wallace, G. G. *Polymer* **1994**, *35*, 3113.
- (9) Majidi, M. R.; Kane-Maguire, L. A. P.; Wallace, G. G. *Polymer* **1995**, *36*, 3597.
- (10) Havinga, E. E.; Bouman, M. M.; Meijer, E. W.; Pomp, A. A.; Simenon, M. M. J. *Synth. Met.* **1994**, *35*, 93.
- (11) Majidi, M. R.; Kane-Maguire, L. A. P.; Wallace, G. G. *Polymer* **1996**, *37*, 359.
- (12) Minto, C. D. G.; Vaughan, A. S. *Polymer*, **1997**, *38*, 2683.
- (13) Majidi, M. R.; Ashraf, S. A.; Kane-Maguire, L. A. P.; Norris, I. D.; Wallace, G. G. *Abstracts, Advances in Polymers III—Designer Polymers, RACI Symposium*, Melbourne, Australia, Sept 1996; pp 12–17.
- (14) Cao, Y.; Qui, J.; Smith, P. *Synth. Met.* **1995**, *69*, 187.
- (15) Neoh, K. G.; Pun, M. Y.; Kang, E. T.; Tan, K. L. *Synth. Met.* **1995**, *73*, 209.
- (16) (a) Chen, S.-A.; Hua, M.-Y. *Macromolecules* **1996**, *29*, 4919 and references cited within. (b) Chen, S.-A.; Hwang, G.-W. *Ibid.* **1996**, *29*, 3950.
- (17) (a) Nguyen, M. T.; Katai, P.; Miller, J. L.; Diaz, A. F. *Macromolecules* **1994**, *27*, 3625. (b) Angelopoulos, M.; Patel, N.; Show, J. M. *Mater. Res. Soc. Symp. Proc.* **1994**, *328*, 173.
- (18) Wei, X.-L.; Wang, Y. Z.; Long, S. M.; Bobeczko, C.; Epstein, A. J. *J. Am. Chem. Soc.* **1997**, *118*, 2545.
- (19) Wang, X.-H.; Li, J.; Jing, X.-B.; Wang, F.-S. *Synth. Met.* **1995**, *69*, 147.
- (20) Armes, S. P. *Polym. News* **1995**, *20*, 233 and references cited therein.
- (21) Vincent, B. *Polym. Adv. Technol.* **1995**, *6*, 356 and refs cited therein.
- (22) Stejskal, J.; Kratochvil, P. *Langmuir* **1996**, *12*, 3389.
- (23) Stejskal, J.; Kratochvil, P.; Armes, S. P.; Lascelles, S. F.; Riede, A.; Helmstedt, M.; Prokeš, J.; Krivka, I. *Macromolecules* **1997**, *30*, 3055.
- (24) Kuramoto, N.; Toita, A. *Polymer* **1997**, *38*, 3055.
- (25) (a) Liao, Y.-H.; Levon, K.; Laakso, J.; Osterholm, J.-E. *Macromol. Rapid Commun.* **1995**, *16*, 393. (b) Fu, Y.; Weiss, R. A. *Macromol. Rapid Commun.* **1996**, *17*, 487.
- (26) Eisazadeh, H.; Spinks, G.; Wallace G. G. *Polymer* **1994**, *35*, 3801.
- (27) Barisci, J. N.; Innis, P. I.; Kane-Maguire, L. A. P.; Norris, I. D.; Wallace G. G. *Synth. Met.* **1997**, *84*, 181.
- (28) (a) Chen, S.-A.; Lee, H.-T., *Synth. Met.* **1992**, *47*, 233. (b) Salanek, W. R.; Lundstrom, I.; Hasan, M. A.; Erlandsson, R.; Konradsson, K.; MacDiarmid, A. G.; Somasiri, N. L. D. In *Electronic Properties of Polymers and Related Compounds*; Kuzmany, H., Mehring, M., Roth, S., Eds.; Springer-Verlag: Berlin, 1985; p 218.
- (29) Norris, I. D.; Kane-Maguire, L. A. P.; Wallace, G. G. Submitted for publication in *Synth. Met.*
- (30) Cao, Y.; Smith, P. *Synth. Met.* **1995**, *69*, 191.
- (31) Pouget, J. P.; Hsu, C.-H.; MacDiarmid, A. G.; Epstein, A. J. *Synth. Met.* **1995**, *69*, 119.

MA9716239